I&EC research
Industrial & Engineering Chemistry Research

Aston University

Kinetics, Catalysis, and Reaction Engineering

Theoretical Analysis of Double Logistic Distributed Activation Energy Model for Thermal Decomposition Kinetics of Solid Fuels

Zhujun Dong, Yang Yang, Wenfei Cai, Yifeng He, Meiyun Chai, Biaobiao Liu, Xi Yu, Scott W. Banks, Xingguang Zhang, Anthony V. Bridgwater, and Junmeng Cai

Just Accepted

ACS Publications

Theoretical Analysis of Double Logistic Distributed Activation Energy

Model for Thermal Decomposition Kinetics of Solid Fuels

Zhujun Dong [a], Yang Yang [b], Wenfei Cai [a], Yifeng He [a], Meiyun Chai [a], Biaobiao Liu [a], Xi Yu [b], Scott

W. Banks [b], Xingguang Zhang [c], Anthony V. Bridgwater [b], Junmeng Cai [a, *]

[a] *Biomass Energy Engineering Research Center, Key Laboratory of Urban Agriculture (South)*

Ministry of Agriculture, School of Agriculture and Biology, Shanghai Jiao Tong University, 800

Dongchuan Road, Shanghai 200240, People's Republic of China

[b] *Bioenergy Research Group, European Bioenergy Research Institute (EBRI), Aston University,*

Birmingham B4 7ET, United Kingdom

[c] *College of Chemical Engineering, Nanjing Forestry University, 159 Longpan Road, Nanjing*

210037, People's Republic of China

Corresponding author: Junmeng Cai. Tel.: +86-21-34206624; E-mail: jmcai@sjtu.edu.cn. Website:

http://biofuels.sjtu.edu.cn

Abstract

The distributed activation energy model (DAEM) has been widely used to analyze the

thermal decomposition of solid fuels such as lignocellulosic biomass and its components, coal,

microalgae, oil shale, waste plastics, and polymer etc. The DAEM with a single distribution

of activation energies cannot describe those reactions well since the thermal decomposition

normally involves multiple sub-processes of various components. The double DAEM

employs a double distribution to represent the activation energies. The Gaussian distribution

is usually used to represent the activation energies. However, it is not sufficiently accurate for

addressing the activation energies in the initial and final stages of the thermal decomposition

reactions of solid fuels. Compared to the Gaussian distribution, the logistic distribution is slightly thicker at the curve tail and suits better to describe the activation energy distribution. In this work, a theoretical analysis of the double logistic DAEM for the thermal decomposition kinetics of solid fuels has been systematically investigated. After the derivation of the double logistic DAEM, its numerical calculation method and the physical meanings of the model parameters have been presented. Three typical types of simulated double logistic DAEM processes have been obtained according to the overlapped situation of two derivative conversion peaks, namely separated, overlapped and partially overlapped processes. It is found that, for the partially overlapped process, the form of the minor peak (overlapped peak or peak shoulder) depends on the values of the frequency factor and heating rate. Considering the simulated processes and related examples from literature, the double logistic DAEM has been remarked as a more reliable tool with abundant flexibility to explain the thermal decomposition of various solid fuels. More accurate results are expected if the double logistic DAEM is coupled with the computational fluid dynamics (CFD) simulation for those reactions mentioned above.

Key words: Distributed activation energy model (DAEM); Solid fuels; Thermal decomposition; Kinetics; Simulation; Logistic distribution

1 Introduction

When solid fuels undergo thermal processing, they decompose and produce gases and volatiles.[1, 2] Depending on the processing temperature and atmosphere, these processes can be classified as pyrolysis, gasification and combustion.[3, 4] Pyrolysis is the thermal decomposition in non-oxidizing environment, resulting in the production of a liquid, solid and gases,[5, 6] and the yields of these products rely on the feedstock and processing conditions.[7, 8] The combustion of solid fuels first undergo endothermic pyrolysis to produce combustible gases,

2

which are subsequently combusted to supply heat required to produce further gases.[9] Gasification is the transformation of solid fuels into a gaseous fuel, which hinges on the gasifying medium on the solid fuels, the temperature and pressure.[10]

A comprehensive understanding of the thermal decomposition kinetics of solid fuels plays an important role in the computational fluid dynamics (CFD) simulation,[11-14] which is a useful tool in reactor design and process optimization.[15-20] Many kinetic models have been proposed to describe the thermal decomposition kinetics of solid fuels.[21-23] The basic model used to describe the thermal decomposition kinetics of biomass components is the single first order reaction (SFOR) model.[24] However, the SFOR model is an empirical model, which is limited to a single reaction process occurring with a single activation energy.[25]

The conventional complex model applied to describe the thermal decomposition kinetics of solid fuels is the distributed activation energy model (DAEM).[13, 26-28] In this model, it is assumed that the thermal decomposition of different components in the solid fuels occurs through a series of reactions with their own activation energies which are described by a continuous distribution function.[29, 30] In general, the activation energy distribution is presented by the Gaussian distribution function. However, it is not sufficiently accurate for addressing the activation energies in the initial and final stages of the thermal decomposition reactions of solid fuels.[31] Cai and co-workers[32] originally proposed to use the logistic distribution to represent the activation energy distribution and successfully applied it for describing cellulose pyrolysis kinetics.[33] The differences between logistic and Gaussian distributions with the same distribution parameters values are presented in Figure 1, which shows that the logistic distribution has slightly thicker tails than the Gaussian distribution, thus offering improved accuracy for describing the thermal decomposition kinetics of solid fuels. Fiori and co-workers [34] found that the logistic DAEM gave a better fitting than the Gaussian DAEM for the pyrolysis kinetics of grape residues. Jain and co-workers[35] concluded that the logistic DAEM matched well with the experimental kinetic curves of coal pyrolysis at different

3

heating rates. Xiong and co-workers[36] simulated the fast pyrolysis of biomass in fluidized bed reactors with a coupled logistic DAEM and CFD model and found that the kinetics with distributed activation energies could affect the predicted average value of the exit vapor-phase tar flux and its statistical distribution, compared to the single-valued activation-energy kinetics. Concerning the chemical kinetic analysis by using the logistic function, Burnham[37] also gave the examples of use and misuse of the logistic function for modeling chemical kinetics and pointed out that some works, such as making comparisons to kinetic parameters derived only with using a single heating rate experiment to fit models, might not qualify as kinetic analysis methods.
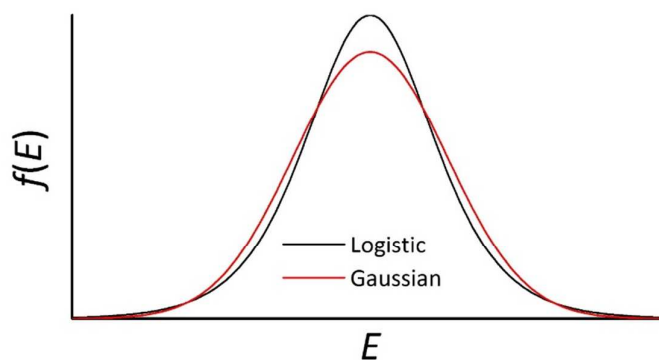
Figure 1. Differences between the logistic and Gaussian distributions with same distribution

parameter values

The thermal decomposition of some solid fuels, such as biomass and coal, usually involves multiple decomposition processes due to varying kinetic behaviors of their components.[38, 39] The DAEM can successfully describe a single process, but difficult to fit multiple sub-processes.[40] Burnham and co-workers[25, 31] developed the kinetics software LLNL (currently Kinetics2015) and proposed some comprehensive models with parallel Gaussian activation energy distributions or combination of the one sigmoidal model and the other Gaussian DAEM for the decomposition of polymers and oil shale. Recently, de Filippis and

4

co-workers[41] proposed the double DAEM, which uses a double distribution function to represent the activation energy distribution. As presented in Supporting Information Table S1, this model was confirmed later as a suitable tool for explaining the pyrolysis kinetic behaviors of microalgae,[40, 42] coal,[35, 40] poly-vinyl chloride (PVC) and poly-methyl methacrylate (PMMA),[43] olive residues,[44] plant oil asphalt[45] and raw and torrefied beech wood xylan samples[46].

The aim of this study is to perform a comprehensive theoretical analysis to the thermal decomposition processes of solid fuels that can be described by the double logistic DAEM. The structure of the paper is arranged as follows. Section 1 provides the background and aim of this work; Section 2 introduces the theory of the double logistic DAEM; Section 3 presents the numerical calculation method for the double logistic DAEM, followed by an investigation of physical meanings of the model parameters in Section 4; Section 5 gives the possible processes related to the thermal decomposition of solid fuels, with discussions on some representative examples in publications; Conclusions of the present work are given in Section 6.

5

2 Double Logistic DAEM

The DAEM can be deduced based on the following assumptions: (1) the decomposition of complex solid fuels contains a large number of independent and parallel first order reactions; (2) each reaction has its own activation energy and all reactions share the same frequency factor; (3) the activation energies of all reactions can be described by a continuous distribution.[26, 31, 32, 47] The equation of the DAEM in the form of conversion can be obtained:

$$\alpha(t) = \int_0^\infty \left\{ 1 - \exp\left[-\int_0^t A\exp\left(-\frac{E}{RT} \right) dt \right] \right\} f(E)\,dE \tag{1}$$

where α is conversion degree (dimensionless), A is the frequency factor (s^{-1}), E is the activation energy (J mol^{-1}), R is the universal gas constant (8.3145 J K^{-1} mol^{-1}), t is the time (s), T is the temperature (K), and $f(E)$ is the activation energy distribution (mol J^{-1}).

The equation of the DAEM in the form of the conversion rate can be obtained by differentiating Equation (1) with respect to t:

$$\frac{d\alpha}{dt}(t) = \int_0^\infty A\exp\left[-\frac{E}{RT} - \int_0^t A\exp\left(-\frac{E}{RT} \right) dt \right] f(E)\,dE \tag{2}$$

The experimental kinetic data is usually obtained under linear heating programs where the temperature increases with time by a constant heating rate.

$$\beta = \frac{dT}{dt} \tag{3}$$

where β is the heating rate (K s^{-1}).

The equations of the DAEM under the linear heating program can be expressed by the following equations (Equations (4) and (5)):

$$\alpha(T) = \int_0^\infty \left\{ 1 - \exp\left[-\frac{A}{\beta}\int_0^T \exp\left(-\frac{E}{RT} \right) dT \right] \right\} f(E)\,dE \tag{4}$$

$$\frac{d\alpha}{dT}(T) = \int_0^\infty \frac{A}{\beta}\exp\left[-\frac{E}{RT} - \frac{A}{\beta}\int_0^T \exp\left(-\frac{E}{RT} \right) dT \right] f(E)\,dE \tag{5}$$

6

The Gaussian distribution function is widely used to represent the activation energy distribution.[26, 48, 49] Whereas it is inappropriate to address the initial and final stages of thermal decomposition of solid fuels. In this regard, the logistic distribution has slightly thicker tails [50] and is reported to be more suitable to describe the thermal decomposition kinetics of solid fuels.[34, 35] Therefore, the logistic distribution for the representation of the activation energies is considered in this work.

In order to better describe the thermal decomposition of solid fuels, which involves two sub-processes, the double logistic distribution is used to represent the activation energy distribution:

$$f(E) = wf_1(E) + (1-w)f_2(E) \tag{6}$$

$$f_1(E) = \frac{\pi}{\sqrt{3}\sigma_1} \frac{\exp\left[-\pi(E-\mu_1)/\left(\sqrt{3}\sigma_1\right)\right]}{\left\{1+\exp\left[-\pi(E-\mu_1)/\left(\sqrt{3}\sigma_1\right)\right]\right\}^2} \tag{7}$$

$$f_2(E) = \frac{\pi}{\sqrt{3}\sigma_2} \frac{\exp\left[-\pi(E-\mu_2)/\left(\sqrt{3}\sigma_2\right)\right]}{\left\{1+\exp\left[-\pi(E-\mu_2)/\left(\sqrt{3}\sigma_2\right)\right]\right\}^2} \tag{8}$$

where w is a constant, $0 < w < 1$, μ is the mean value (J mol^{-1}) and σ is the standard deviation (J mol^{-1}) of the activation energy distribution, the subscripts 1 and 2 represent the values related to the first and second sub-processes.

3 Numerical calculation

There are an inner dT integral and an outer dE integral in Equations (4) or (5), which result in difficulties in solving them. For this reason, a numerical approach for calculating the DAEM is developed in this section.

In fact, the inner dT integral is the temperature integral,[51-53] which can be expressed in the following form:

7

$$\int_0^T \exp\left(-\frac{E}{RT}\right) dT = \frac{E}{R} \int_{E/(RT)}^{\infty} \frac{\exp(-x)}{x^2} dx = \frac{E}{R} P\left(\frac{E}{RT}\right) \tag{9}$$

$$p\left(\frac{E}{RT}\right) = \frac{\exp[-E/(RT)]}{E/(RT)} - \int_{E/(RT)}^{\infty} \frac{\exp(-x)}{x} dx \tag{10}$$

In mathematics, there is a special integral named the exponential integral:

$$\mathrm{Ei}(x) = -\int_{-x}^{\infty} \frac{e^{-t}}{t} dt \tag{11}$$

The exponential integral can be easily solved by using a specific function "ExpIntegralEi" in the Mathematica software system.[54] Substituting Equations (10) and (11) into Equation (9) results in

$$\int_0^T \exp\left(-\frac{E}{RT}\right) dT = T \exp\left(-\frac{E}{RT}\right) + \frac{E}{R} \mathrm{Ei}\left(-\frac{E}{RT}\right) \tag{12}$$

As for the outer $\mathrm{d}E$ integral, the upper integration limit is ∞. According to Güneş and Güneş,[55] if the upper integration limit is replaced by a value high enough, there is almost no deviation from the real value. The effect of different upper integration limits ($\mu+3\sigma$, $\mu+10\sigma$ and $\mu+30\sigma$, where μ is the greater one of μ_1 and μ_2, σ is the greater one of σ_1 and σ_2) on the numerical results of the double logistic DAEM was investigated and shown in **Figure 2**. It can be observed that the $\mathrm{d}\alpha/\mathrm{d}T - T$ curves would converge into a curve with increasing of upper integration limit values. Since there was almost no deviation from the final converge curve when the upper integration limit increased to $\mu+10\sigma$, $\mu+10\sigma$ is selected as the upper integration limit of the outer $\mathrm{d}E$ integral for further calculation of the double logistic DAEM. Then, the outer $\mathrm{d}E$ integral can be converted to a normal definite integral, as shown in Equations (13) and (14).

$$\begin{aligned}
\alpha(T) &= \int_0^{\infty} \left\{ 1 - \exp\left[-\frac{A}{\beta} \frac{E}{R} P\left(\frac{E}{RT}\right) \right] \right\} f(E) \mathrm{d}E \\
&\approx \int_0^{\mu+10\sigma} \left\{ 1 - \exp\left[-\frac{A}{\beta} \frac{E}{R} P\left(\frac{E}{RT}\right) \right] \right\} f(E) \mathrm{d}E
\end{aligned} \tag{13}$$

8

$$\frac{d\alpha}{dT}(T) = \int_0^\infty \frac{A}{\beta}\exp\left[-\frac{E}{RT} - \frac{A}{\beta}\frac{E}{R}P\left(\frac{E}{RT}\right)\right]f(E)\,dE$$

$$\approx \int_0^{\mu+10\sigma} \frac{A}{\beta}\exp\left[-\frac{E}{RT} - \frac{A}{\beta}\frac{E}{R}P\left(\frac{E}{RT}\right)\right]f(E)\,dE$$

(14)

For numerical calculations of Equations (13) and (14), Simpson's rule,[56] a common method for numerical integration, was used. **Figure 3** shows the numerical calculation flowchart of the double logsitic DAEM.
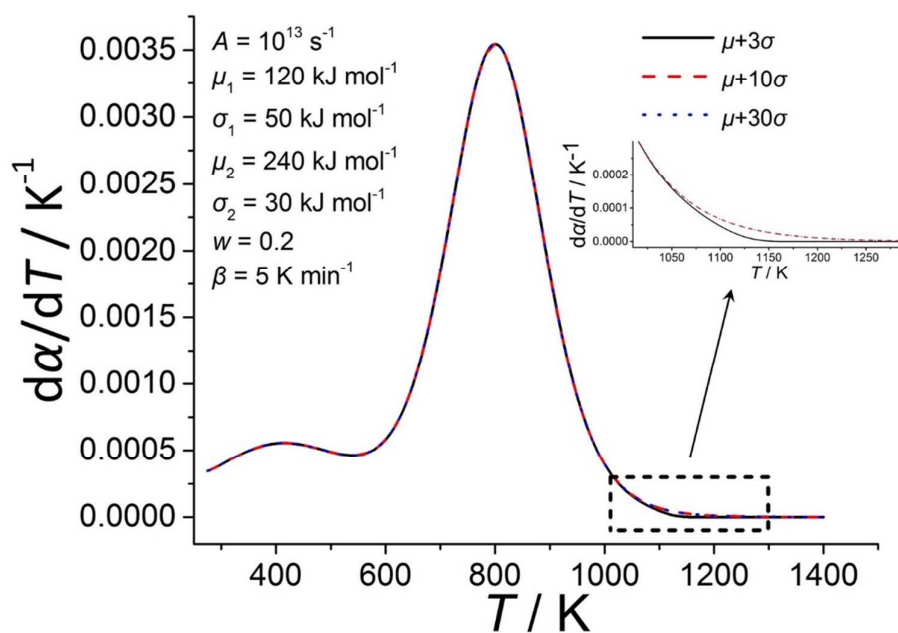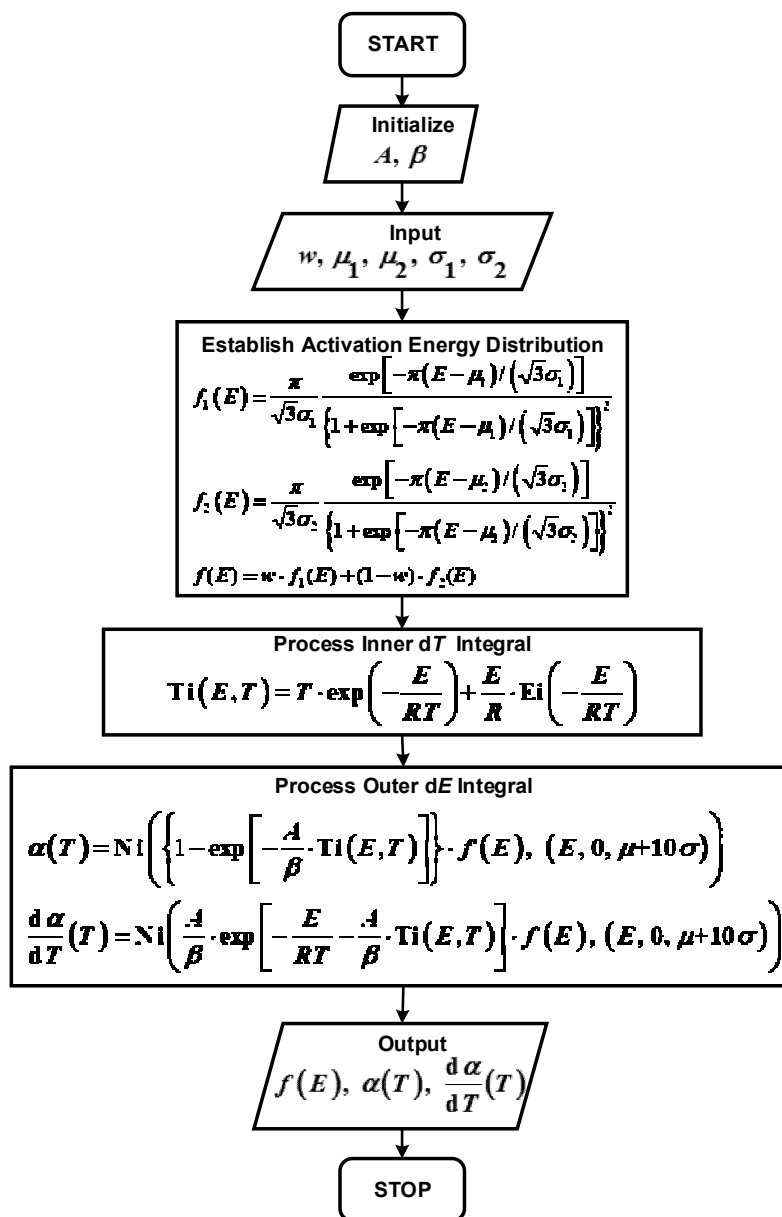

Figure 2. Effect of upper intergration limit on numerical results of double logistic DAEM

Figure 3. Numeical calcualtion flowchart of double logistic DAEM (Ei: Exponential integral;

Ti: Temperature integral; Ni: Numerical integration function)

4 Physical meaning of model parameters

The influences of various parameters on α for the Gaussian DAEM can be found in our previous study. [57] In fact, the $d\alpha/dT$ data is more sensitive to reveal model details.[58, 59] Therefore, in this section, the influences of the model parameters on the $d\alpha/dT - T$ curve are

investigated and the physical meanings of model parameters are presented.

Substituting Equation (6) into Equations (4) and (5) leads to:

$$
\begin{aligned}
\alpha(T) &= w \cdot \int_0^\infty \left\{ 1 - \exp\left[-\frac{A}{\beta} \int_0^T \exp\left(-\frac{E}{RT}\right) dT \right] \right\} f_1(E) dE \\
&\quad + (1-w) \cdot \int_0^\infty \left\{ 1 - \exp\left[-\frac{A}{\beta} \int_0^T \exp\left(-\frac{E}{RT}\right) dT \right] \right\} f_2(E) dE \quad (15) \\
&= w \cdot \alpha_1(T) + (1-w) \cdot \alpha_2(T)
\end{aligned}
$$

$$
\begin{aligned}
\frac{d\alpha}{dT}(T) &= w \cdot \int_0^\infty \frac{A}{\beta} \exp\left[-\frac{E}{RT} - \frac{A}{\beta} \int_0^T \exp\left(-\frac{E}{RT}\right) dT \right] f_1(E) dE \\
&\quad + (1-w) \cdot \int_0^\infty \frac{A}{\beta} \exp\left[-\frac{E}{RT} - \frac{A}{\beta} \int_0^T \exp\left(-\frac{E}{RT}\right) dT \right] f_2(E) dE \quad (16) \\
&= w \cdot \frac{d\alpha_1}{dT}(T) + (1-w) \cdot \frac{d\alpha_2}{dT}(T)
\end{aligned}
$$

From Equations (15) and (16), it can be obtained that the double DAEM can be considered as the weighted sum of two single DAEMs and w is the weight parameter. **Figure 4** shows the influences of w on the numerical results of the double logistic distribution and the double logistic DAEM. It can be also elucidated that w can affect the height of each $d\alpha/dT$ peak from **Figure 4**.
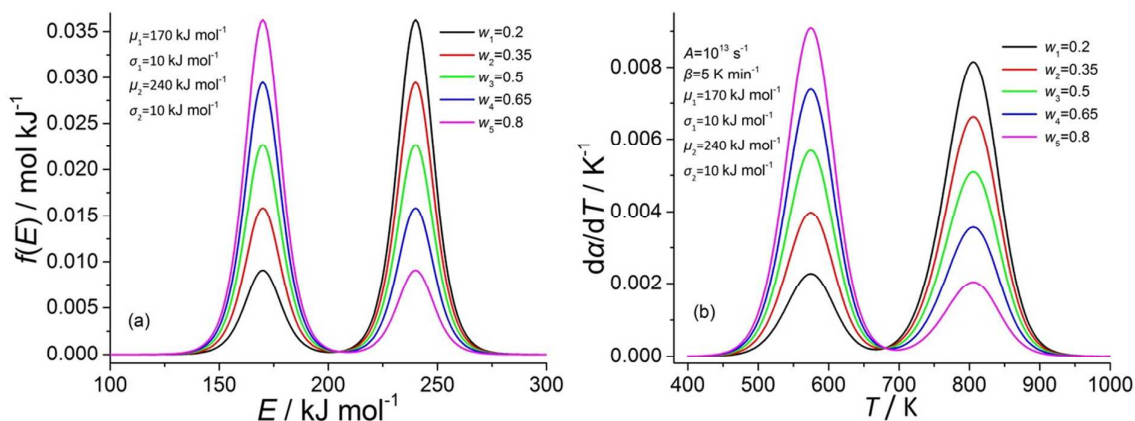

Figure 4. Effect of w on numerical results of (a) double logistic distribution and (b) double logistic DAEM

11

Since the double DAEM is considered as the weighted sum of two single DAEMs, the single DAEM can be used to investigate the physical meaning of μ and σ in the logistic DAEM. The study is carried out by changing each parameter, taking one parameter at a time and keeping the remaining parameters unchanged.

Figure 5 shows the effect of μ on the numerical results of the logistic distribution and the logistic DAEM. It can be observed that increasing μ can result in the change of the $d\alpha/dT$ peak location. Along with the increase of μ, the $d\alpha/dT$ - T curve is shifted to higher temperature. This is consistent with the kinetic theory that the higher activation energy needs higher temperature to trigger the reaction.[60, 61] Therefore, μ can be considered as the location parameter in the logistic DAEM while increasing μ may cause a decrease in $d\alpha/dT$ peak height.
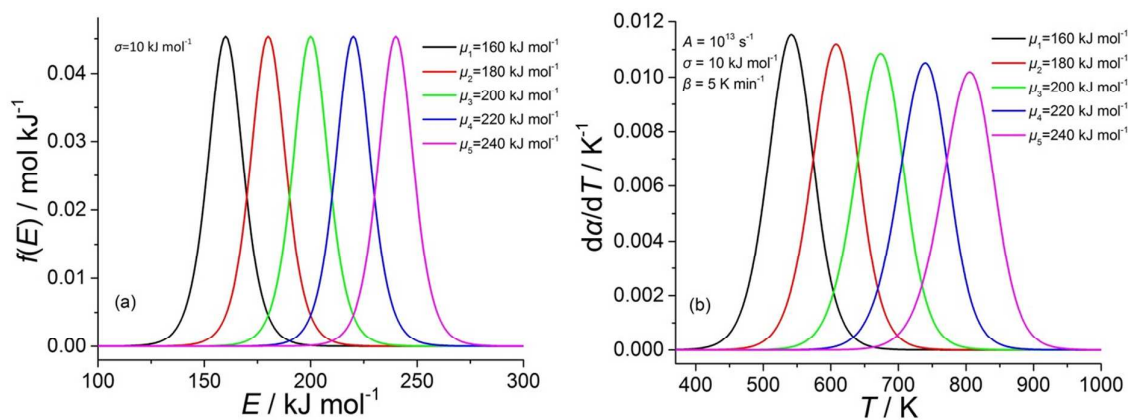

Figure 5. Effect of μ on numerical results of (a) logistic distribution and (b) logistic DAEM

Figure 6 shows the effect of σ on the numerical results of the logistic distribution and the logistic DAEM. It can be observed that increasing σ exerts significant effect on the $d\alpha/dT$ peak height while the $d\alpha/dT$ - T curve becomes broader and shallower with increasing σ. Therefore, σ can be suggested as the shape parameter of the logistic DAEM.
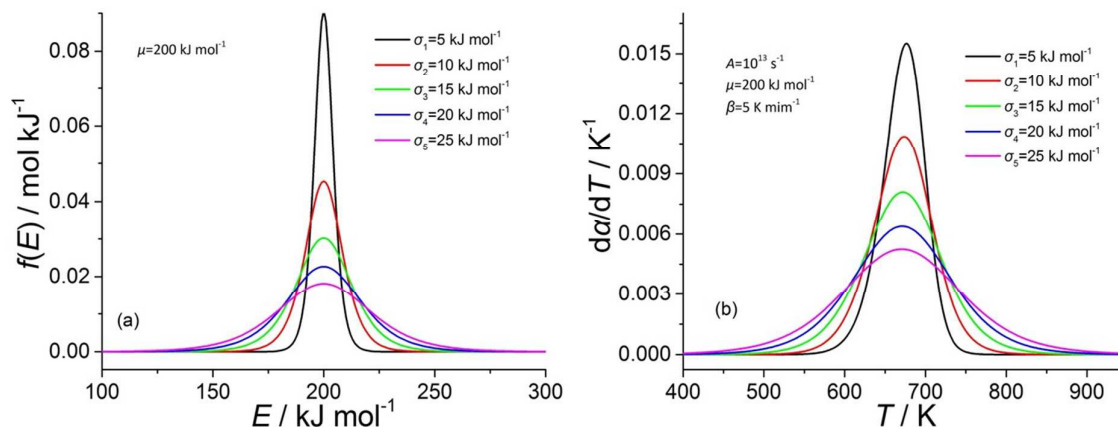
12

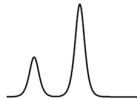**Figure 6.** Effect of σ on numerical results of (a) logistic distribution and (b) logistic DAEM
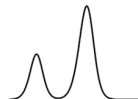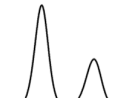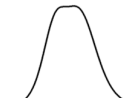
5 Typical double logistic DAEM processes
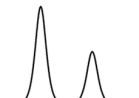
To present a wide range of thermal decomposition processes, some theoretical double logistic DAEM processes are simulated. All simulated $\alpha - T$ and $d\alpha/dT - T$ curves are calculated in 10,000 temperature points (300 K $\leq T \leq$ 1300 K). According to a series of pre-calculations, it was found that the shape of the $d\alpha/dT$ curve mainly depends on the shape of the corresponding double logistic distribution, like μ_1, μ_2, σ_1, σ_2 and w. According to the results about the double distribution from Robertson and co-workers,[62] the distribution shape depends on the values of the following three parameters: w, $r=\sigma_2/\sigma_1$ and $u=(\mu_2-\mu_1)/\sigma_1$ when the modality of the distribution shape is unaffected by location and scale changes. Based on the above conclusion, without loss of generality, the parameters μ_2 and σ_2 are set as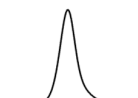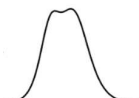 fixed values ($\mu_2 = 240$ kJ mol^{-1} and $\sigma_2 = 20$ kJ mol^{-1}) for the simulation of the double logistic DAEM processes. The values of the other parameters were set as follows: μ_1 (from 120 to 240 kJ mol^{-1} with an interval of 10 kJ mol^{-1}), σ_1 (from 1.0 to 50.0 kJ mol^{-1} with an interval of 1.0 kJ mol^{-1}), A (from 10^{11} to 10^{21} s^{-1} with a ratio of 10), w (from 0.2 to 0.8 with an interval of 0.05)

13

and β (from 0.125 to 128 K min^{-1}).

According to the shapes of the simulated dα/dT curves, those simulated double logistic DAEM processes can be divided into three types: (1) separated process; (2) overlapped process; and (3) partially overlapped process. The corresponding $f(E)$, $\alpha - T$ and dα/d$T - T$ curves are listed in **Table 1**. Some examples of the thermal decomposition of solid fuels corresponding to the above typical processes are also presented in **Table 1**.

14

Table 1. Typical processes described by double logistic DAEM

No.	Name	Typical curves			Characteristics	Examples from literature
		$f(E)$ curve	$\alpha - T$ curve	$d\alpha/dT - T$ curve		
1	Separated process				• There are two significantly separate peaks in the dα/dT curve. • The left peak value is lower than the right peak value.	Pyrolysis of oil shale [49]
					• There are two significantly separate peaks in the dα/dT curve. • The left peak value is higher than the right peak value.	Gasification of municipal solid waste (MSW) under 80%N_2/20%CO_2 atmosphere [63] Pyrolysis of poly-vinyl chloride (PVC) [43]
2	Overlapped process				• There is one sharp peak in the dα/dT curve.	Combustion of coal and biomass char blends [64]
					• There is one flat peak in the dα/dT curve.	

15

3	Partially overlapped process		• There are two partially overlapped peaks in the dα/dT curve. • The left peak value is lower than the right peak value.	Pyrolysis of Russian coal (anthracite) [41]
			• There are two partially overlapped peaks in the dα/dT curve. • The left peak value is higher than the right peak value.	Pyrolysis of Sulcis coal (Italian sub-bituminous coal) [41]
			• There is one peak in the dα/dT curve. • There is a peak shoulder in the left side of the peak.	Pyrolysis of cotton stalk, pine wood and wheat straw (lignocellulosic biomass) [30] Pyrolysis of plant oil asphalt [45] Pyrolysis of poly-methyl methacrylate (PMMA) [43]
			• There is one peak in the dα/dT curve. • There is a peak shoulder in the right side of the peak.	Pyrolysis of microalgae [42]

16

(1) Separated processes

The main characteristic of the first type is that there are two separate peaks in the $d\alpha/dT$ curve. In this type of process, there are two distinguishable sub-processes, which occur in completely different temperature ranges.

There were several examples corresponding to this type of process in publications. Tiwari and Deo[49] investigated the pyrolysis of oil shale, which involved the organic and carbonate decomposition. The organic decomposition has been reported between 250 and 500 ℃ while the carbonate decomposition commenced at 525 ℃ or above depending on the heating rate. In addition, the derivative conversion curves of oil shale pyrolysis showed two separate peaks. Lai and co-workers[63] performed the gasification kinetics of municipal solid waste (MSW) under $80\%N_2/20\%CO_2$ atmosphere. The derivative conversion curves showed two separate peaks, which corresponded to the thermal decomposition of MSW from 200 to 650 ℃, and the reaction between CO_2 and the char production at above 700 ℃. Following the above conclusion, the derivative conversion curves of biomass gasification process will generate two separate peaks, which corresponded to the thermal decomposition of biomass (drying and pyrolysis, < 650 ℃), and the reaction between fuel gas (syngas, CO_2, steam) and hot reactive charcoal above 650 ℃. Bhargava and co-workers[43] performed the pyrolysis of poly vinyl chloride (PVC). The resulting derivative conversion curves at different heating rates showed two separate peaks, which were mainly attributed to the release of hydrogen chloride and the formation of aliphatic, olefinic and aromatic hydrocarbons and char, respectively.

According to the simulation results obtained in this work, if the value of

$$\frac{|\mu_1 - \mu_2|}{\sqrt{\sigma_1^2 + \sigma_2^2}}$$ is high enough (the critical value depends on the values of A and β), the

17

double logistic DAEM shows two separate peaks, which is consistent with the results from Ashman and co-workers[65] for the double normal distribution.

(2) Overlapped processes

When the difference between the mean values of two distribution components, $|\mu_1 - \mu_2|$, is small, the double logistic DAEM shows one single peak in the $d\alpha/dT$ curve. Researchers usually used certain single process kinetic models (such as the SFOR model or the single DAEM) to describe this type of process.

Moyo[64] performed the combustion kinetic analysis of a blend of 50% biomass char and 50% coal char. The derivative conversion curves at different heating rates (8, 12 and 15 K min^{-1}) showed a single peak, which was attributed to the fact that the combustion kinetic behaviors of biomass char and coal char were similar.

(3) Partially overlapped processes

This type can describe the process which involves two partially overlapped sub-processes. The curve shows a main peak with a minor peak appearing as an overlapped peak or a peak shoulder.

The form of overlapped peak or peak shoulder depends on the values of A and β, except w, r and u. **Figure 7 (a)** shows an example of the effect of A on the $d\alpha/dT - T$ curve of the double logistic DAEM. It can be observed that the form of the minor peak varies from the peak shoulder to the overlapped peak when the value of A increases from 10^{11} to 10^{21} s^{-1}. The increase of the frequency factor shifts the $d\alpha/dT - T$ curve to the left side. An example of the effect of β on the $d\alpha/dT - T$ curve of the double logistic DAEM is presented in **Figure 7 (b),** where the minor peak varies from the overlapped peak to the peak shoulder with an increasing value of β from 0.125 to 128 K min^{-1}. As β increases, the $d\alpha/dT - T$ curve is shifted to higher temperatures, but the $d\alpha/dT$ peak height decreases.

18
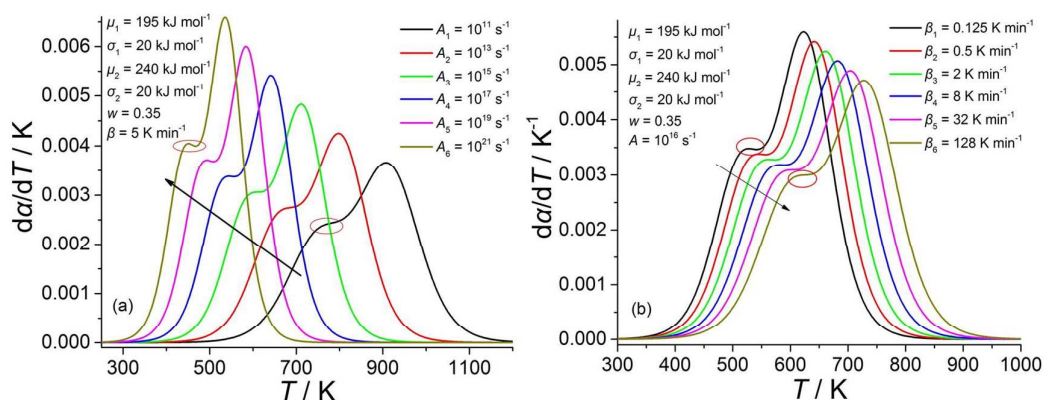
Figure 7. Examples of effects of (a) *A* and (b) *β* on the d*α*/d*T* – *T* curve of the double

logistic DAEM

Many examples of the thermal decomposition of solid fuels from literature

belongs to this type of process.

Cai and co-workers[30] conducted the pyrolysis of eight lignocellulosic feedstocks

and presented the corresponding derivative conversion curves had a main peak and a

peak shoulder on the left side of the main peak. The main peak corresponded to the

pyrolysis of cellulose, while the peak shoulder on the left side of the main peak

corresponded to the pyrolysis of hemicellulose.[66] Tang and co-workers[45] performed

the pyrolysis kinetics of plant oil asphalt, a lipid-based residue biomass generated in

biodiesel and fatty acid industries. The corresponding derivative conversion curves

had a main peak with a left peak shoulder which corresponded to the pyrolysis of two

pseudo-components, respectively. In contrast, de Filippis and co-workers[40, 42] found

that the derivative conversion curve presented a main peak with a peak shoulder on its

right side during the pyrolysis of microalgae. The breakage of the weakest chemical

bonds in microalgae has been reported during the primary pyrolysis sub-process,

whereas the secondary pyrolysis sub-process favors the rupturing of stronger bonds

19

and releases the hydrogen from the aromatic and aliphatic groups. Bhargava and co-workers [43] investigated the pyrolysis of poly-methyl methacrylate (PMMA) and found a main broad peak and a minor peak shoulder on the left side of the main peak, which was attributed to the reactions occurring at the chain ends and random scission process producing only monomers. In the kinetic study of coal pyrolysis from de Caprariis and co-workers[41], the derivative conversion curves at different heating rates showed two partially overlapped peaks, which corresponded to a primary and secondary pyrolysis sub-processes, respectively. Light volatiles and tar were released in the primary pyrolysis sub-process while the repolymerization of coal molecules to produce char took place in the secondary pyrolysis sub-process.[40]

According to aforementioned theoretical analyses, the double logistic DAEM can be suggested as the most suitable tool for explaining the pyrolysis, combustion, or gasification of various solid fuels which involve two thermal decomposition sub-processes. When double logistic DAEM is applied to describe thermal decomposition of solid fuels, the model parameters (A, μ_1, μ_2, σ_1 and σ_2) will provide information about the activation energy distribution of each sub-process and weights of both sub-processes. In the future work, these parameters will also be investigated with optimization tools. It can be expected that the simulation results of the thermal decomposition of solid fuels should fit the experimental data more accurately if the double logistic DAEM would be coupled with the CFD simulation.

6 Conclusions

- The equations of the double logistic DAEM were obtained and shown in Equations (4)-(8).

- The numerical calculation of the double logistic DAEM can be performed by the

20

following method: the inner dT integral can be expressed in the form of the exponential integral which can be easily processed in some mathematical software systems, and the outer dE integral can be numerically solved by using Simpson's rule.

- The double logistic DAEM is the weighted sum of two single logistic DAEMs and the parameter w is the weight parameter. The parameters μ_1 and μ_2 are the location parameters and mainly affect the locations of the dα/d$T - T$ curve peaks. The parameters σ_1 and σ_2 are the shape parameters and mainly determine the shape of the dα/d$T - T$ curve.

- Three typical types of simulated double logistic DAEM processes were obtained: separated, overlapped and partially overlapped processes.

  (1) When the value of $\dfrac{|\mu_1 - \mu_2|}{\sqrt{\sigma_1^2 + \sigma_2^2}}$ is high enough, the dα/d$T - T$ curve of the double logistic DAEM shows two separate peaks.

  (2) If the difference between the mean values ($|\mu_1 - \mu_2|$) of two distribution components is small, the double logistic DAEM shows one single peak in the dα/dT curve.

  (3) As for the overlapped process, the form of the minor peak is the overlapped peak or peak shoulder depending on the values of A and β.

- The double logistic DAEM is a suitable tool with abundant flexibility in explaining the thermal decomposition of solid fuels, such as the pyrolysis, combustion or gasification of various solid fuels (e.g. lignocellulosic biomass, coal, microalgae, plant oil asphalt, plastics).

- The analysis of experimental kinetic data by using the double DAEM as well as the comparison between the logistic and Gaussian distributions in DAEM will be

21

our next work. It is hoped that our work can help to establish a comprehensive research framework for the double logistic DAEM.

Acknowledgements

Supporting Information

Further details on the application of the double DAEM in thermal decomposition kinetics of solid fuels from literature.

The authors declare no competing financial interest.

Nomenclature

Acronyms

DAEM	Distributed activation energy model
CFD	Computational fluid dynamics
SFOR	Single first order reaction
PVC	Poly-vinyl chloride
PMMA	Poly-methyl methacrylate
MSW	Municipal solid waste

22

TGA	Thermo-gravimetric analysis
Ei	Exponential integral
Ti	Temperature integral
Ni	Numerical integration function

Variables

α	Conversion degree (dimensionless)
A	Frequency factor (s^{-1})
E	Activation energy (J mol^{-1})
R	Universal gas constant (8.3145 J K^{-1} mol^{-1})
t	Time (s)
T	Temperature (K)
$f(E)$	Activation energy distribution (mol J^{-1})
β	Heating rate (K s^{-1})
w	Constant, $0 < w < 1$
μ	Mean value of $f(E)$ (J mol^{-1})
σ	Standard deviation of $f(E)$ (J mol^{-1})

Subscript

1	Values related to the first sub-processes
2	Values related to the second sub-processes

References

1. Laird, D. A.; Brown, R. C.; Amonette, J. E.; Lehmann, J., Review of the pyrolysis platform for coproducing bio-oil and biochar. *Biofuels, Bioprod. Biorefin.* **2009,** 3, (5), 547-562.

2. Mohan, D.; Pittman, C. U.; Steele, P. H., Pyrolysis of wood/biomass for bio-oil: A critical review. *Energy Fuels* **2006,** 20, (3), 848--889.

3. Zhang, J.; Wu, R.; Zhang, G.; Yu, J.; Yao, C.; Wang, Y.; Gao, S.; Xu, G., Technical review on thermochemical conversion based on decoupling for solid carbonaceous fuels. *Energy Fuels* **2013,** 27, (4), 1951-1966.

4.   Kumar, G.; Shobana, S.; Chen, W. H.; Bach, Q. V.; Kim, S. H.; Atabani, A. E.; Chang, J. S., A review of thermochemical conversion of microalgal biomass for biofuels: Chemistry and processes. *Green Chem.* **2017,** 19, (1), 44-67.

5.   Yu, Y.; Yang, Y.; Cheng, Z.; Blanco, P. H.; Liu, R.; Bridgwater, A. V.; Cai, J., Pyrolysis of rice husk and corn stalk in auger reactor. 1. Characterization of char and gas at various temperatures. *Energy Fuels* **2016,** 30, (12), 10568-10574.

6.   Cai, J.; Banks, S. W.; Yang, Y.; Darbar, S.; Bridgwater, T., Viscosity of aged bio-oils from fast pyrolysis of beech wood and miscanthus: Shear rate and temperature Dependence. *Energy Fuels* **2016,** 30, (6), 4999-5004.

7.   Kan, T.; Strezov, V.; Evans, T. J., Lignocellulosic biomass pyrolysis: A review of product properties and effects of pyrolysis parameters. *Renewable Sustainable Energy Rev.* **2016,** 57, 1126-1140.

8.   Huber, G. W.; Iborra, S.; Corma, A., Synthesis of transportation fuels from biomass: Chemistry, catalysts, and engineering. *Chem. Rev.* **2006,** 106, (9), 4044-98.

9.   Wang, J.; Anthony, E. J., Clean combustion of solid fuels. *Appl. Energy* **2008,** 85, (2–3), 73-79.

10. de Souza-Santos, M. L., *Solid Fuels Combustion and Gasification: Modeling, Simulation, and Equipment Operations Second Edition*. CRC Press: 2010.

11. Di Blasi, C., Modeling chemical and physical processes of wood and biomass pyrolysis. *Prog. Energy Combust. Sci.* **2008,** 34, (1), 47-90.

12. Sharma, A.; Pareek, V.; Zhang, D., Biomass pyrolysis—A review of modelling, process parameters and catalytic studies. *Renewable Sustainable Energy Rev.* **2015,** 50, 1081-1096.

13. Hough, B. R.; Beck, D. A. C.; Schwartz, D. T.; Pfaendtner, J., Application of machine learning to pyrolysis reaction networks: Reducing model solution time to

24

enable process optimization. *Comput. Chem. Eng.* **2017,** 104, 56-63.

14. Xiong, Q.; Yang, Y.; Xu, F.; Pan, Y.; Zhang, J.; Hong, K.; Lorenzini, G.; Wang, S., Overview of computational fluid dynamics simulation of reactor-scale biomass Pyrolysis. *ACS Sustainable Chem. Eng.* **2017,** 5, (4), 2783-2798.

15. Zhang, J.; Chen, T.; Wu, J.; Wu, J., Multi-Gaussian-DAEM-reaction model for thermal decompositions of cellulose, hemicellulose and lignin: comparison of N_2 and CO_2 atmosphere. *Bioresour. Technol.* **2014,** 166, (8), 87-95.

16. White, J. E.; Catallo, W. J.; Legendre, B. L., Biomass pyrolysis kinetics: A comparative critical review with relevant agricultural residue case studies. *J. Anal. Appl. Pyrolysis* **2011,** 42, (31), 1-33.

17. Czajka, K.; Kisiela, A.; Moroń, W.; Ferens, W.; Rybak, W., Pyrolysis of solid fuels: Thermochemical behaviour, kinetics and compensation effect. *Fuel Process. Technol.* **2016,** 142, 42-53.

18. Yu, X.; Makkawi, Y.; Ocone, R.; Huard, M.; Briens, C.; Berruti, F., A CFD study of biomass pyrolysis in a downer reactor equipped with a novel gas–solid separator - I: Hydrodynamic performance. *Fuel Process. Technol.* **2014,** 126, 366-382.

19. Yu, X.; Hassan, M.; Ocone, R.; Makkawi, Y., A CFD study of biomass pyrolysis in a downer reactor equipped with a novel gas–solid separator - II: Thermochemical performance and products. *Fuel Process. Technol.* **2015,** 133, (126), 51-63.

20. Anca-Couce, A., Reaction mechanisms and multi-scale modelling of lignocellulosic biomass pyrolysis. *Prog. Energy Combust. Sci.* **2016,** 53, 41-79.

21. White, J. E.; Catallo, W. J.; Legendre, B. L., Biomass pyrolysis kinetics: A comparative critical review with relevant agricultural residue case studies. *Journal of Analytical and Applied Pyrolysis* **2011,** 91, (1), 1-33.

22. de Souza-Santos, M. L., *Solid Fuels Combustion and Gasification: Modeling,*

Simulation, and Equipment Operations (Second Edition). CRC Press: 2010.

23. Wang, S.; Ru, B.; Lin, H.; Dai, G.; Wang, Y.; Luo, Z., Kinetic study on pyrolysis of biomass components: A critical review. *Curr. Org. Chem.* **2016,** 20, (999), 2489 - 2513.

24. Urych, B., Determination of Kinetic Parameters of Coal Pyrolysis to Simulate the Process of Underground Coal Gasification (UCG). *J. Sustainable Min.* **2014,** 13, (1), 3-9.

25. Burnham, A. K., *Global Chemical Kinetics of Fossil Fuels: How to Model Maturation and Pyrolysis*. Springer International Publishing: 2017.

26. Cai, J.; Wu, W.; Liu, R., An overview of distributed activation energy model and its application in the pyrolysis of lignocellulosic biomass. *Renewable Sustainable Energy Rev.* **2014,** 36, 236-246.

27. Li, X.; Mei, Q.; Dai, X.; Ding, G., Effect of anaerobic digestion on sequential pyrolysis kinetics of organic solid wastes using thermogravimetric analysis and distributed activation energy model. *Bioresour. Technol.* **2017,** 227, 297-307.

28. Stankovic, B.; Jovanovic, J.; Ostojic, S.; Adnadjevic, B., Kinetic analysis of non-isothermal dehydration of poly(acrylic acid)-g-gelatin hydrogel using distributed activation energy model. *J. Therm. Anal. Calorim.* **2017,** 129, (1), 541-551.

29. Cai, J.; Liu, R., New distributed activation energy model: Numerical solution and application to pyrolysis kinetics of some types of biomass. *Bioresour. Technol.* **2008,** 99, (8), 2795-9.

30. Cai, J.; Wu, W.; Liu, R.; Huber, G. W., A distributed activation energy model for the pyrolysis of lignocellulosic biomass. *Green Chem.* **2013,** 15, (5), 1331-1340.

31. Burnham, A. K., Global kinetic analysis of complex materials. *Energy Fuels* **1999,** 13, (1), 1-22.

32. Cai, J.; Jin, C.; Yang, S.; Chen, Y., Logistic distributed activation energy model – Part 1: Derivation and numerical parametric study. *Bioresour. Technol.* **2011,** 102, (2), 1556-61.

33. Cai, J.; Yang, S.; Li, T., Logistic distributed activation energy model – Part 2: Application to cellulose pyrolysis. *Bioresour. Technol.* **2011,** 102, (3), 3642-3644.

34. Fiori, L.; Valbusa, M.; Lorenzi, D.; Fambri, L., Modeling of the devolatilization kinetics during pyrolysis of grape residues. *Bioresour. Technol.* **2012,** 103, (1), 389-397.

35. Jain, A. A.; Mehra, A.; Ranade, V. V., Processing of TGA data: Analysis of isoconversional and model fitting methods. *Fuel* **2016,** 165, 490-498.

36. Xiong, Q.; Zhang, J.; Xu, F.; Wiggins, G.; Stuart Daw, C., Coupling DAEM and CFD for simulating biomass fast pyrolysis in fluidized beds. *J. Anal. Appl. Pyrolysis* **2016,** 117, 176-181.

37. Burnham, A. K., Use and misuse of logistic equations for modeling chemical kinetics. *J. Therm. Anal. Calorim.* **2017,** 127, (1), 1107-1116.

38. Epshtein, S. A.; Kossovich, E. L.; Kaminskii, V. A.; Durov, N. M.; Dobryakova, N. N., Solid fossil fuels thermal decomposition features in air and argon. *Fuel* **2017,** 199, 145-156.

39. Dhyani, V.; Bhaskar, T., A comprehensive review on the pyrolysis of lignocellulosic biomass. *Renewable Energy* **2017**, doi: 10.1016/j.renene.2017.04.035.

40. De Filippis, P.; de Caprariis, B.; Scarsella, M.; Verdone, N., Double Distribution Activation Energy Model as Suitable Tool in Explaining Biomass and Coal Pyrolysis Behavior. *Energies* **2015,** 8, (3), 1730-1744.

41. de Caprariis, B.; de Filippis, P.; Herce, C.; Verdone, N., Double-Gaussian distributed activation energy model for coal devolatilization. *Energy Fuels* **2012,** 26,

(26), 6153–6159.

42. de Filippis, P.; de Caprariis, B.; Scarsella, M.; Verdone, N. In *Double distribution activation energy model for microalgae pyrolysis*, The 5th International Conference on Development, Energy, Environment, Economics, Florence, Italy, November 22-24, 2014; Florence, Italy, 2014; pp 68-73.

43. Bhargava, A.; van Hees, P.; Andersson, B., Pyrolysis modeling of PVC and PMMA using a distributed reactivity model. *Polym. Degrad. Stab.* **2016,** 129, 199-211.

44. de Caprariis, B.; Santarelli, M. L.; Scarsella, M.; Herce, C.; Verdone, N.; De Filippis, P., Kinetic analysis of biomass pyrolysis using a double distributed activation energy model. *J. Therm. Anal. Calorim.* **2015,** 121, (3), 1403-1410.

45. Tang, Q.; Zheng, Y.; Wang, T.; Wang, J., Study on the kinetics of plant oil asphalt pyrolysis using thermogravimetry and the distributed activation energy model. *Energy Fuels* **2014,** 28, (3), 2035-2040.

46. Wang, S.; Dai, G.; Ru, B.; Zhao, Y.; Wang, X.; Zhou, J.; Luo, Z.; Cen, K., Effects of torrefaction on hemicellulose structural characteristics and pyrolysis behaviors. *Bioresour. Technol.* **2016,** 218, 1106-14.

47. Bhavanam, A.; Sastry, R. C., Kinetic study of solid waste pyrolysis using distributed activation energy model. *Bioresour. Technol.* **2015,** 178, 126-131.

48. Wu, W.; Cai, J.; Liu, R., Isoconversional kinetic analysis of distributed activation energy model processes for pyrolysis of solid fuels. *Ind. Eng. Chem. Res.* **2013,** 52, (40), 14376-14383.

49. Tiwari, P.; Deo, M., Detailed kinetic analysis of oil shale pyrolysis TGA data. *AIChE J.* **2012,** 58, (2), 505-515.

50. Meeker, W. Q.; Escobar, L. A., *Statistical Methods for Reliability Data*. Wiley:

28

2014.

51. Órfão, J. J. M., Review and evaluation of the approximations to the temperature integral. *AIChE J.* **2007,** 53, (11), 2905-2915.

52. Cai, J.; Yao, F.; Yi, W.; He, F., New temperature integral approximation for nonisothermal kinetics. *AIChE J.* **2006,** 52, (4), 1554–1557.

53. Deng, C.; Cai, J.; Liu, R., Kinetic analysis of solid-state reactions: Evaluation of approximations to temperature integral and their applications. *Solid State Sci.* **2009,** 11, (8), 1375-1379.

54. Wellin, P., *Programming with Mathematica®: An Introduction.* Cambridge University Press: 2013.

55. Güneş, M.; Güneş, S., The influences of various parameters on the numerical solution of nonisothermal DAEM equation. *Thermochim. Acta* **1999,** 336, (1–2), 93-96.

56. Epperson, J. F., *An Introduction to Numerical Methods and Analysis*. John Wiley & Sons: 2007.

57. Cai, J.; He, F.; Yao, F., Nonisothermal *n*th-order DAEM equation and its parametric study – use in the kinetic analysis of biomass pyrolysis. *J. Math. Chem.* **2007,** 42, (4), 949-956.

58. Carrier, M.; Auret, L.; Bridgwater, A.; Knoetze, J. H., Using apparent activation energy as a reactivity criterion for biomass pyrolysis. *Energy Fuels* **2016,** 30, (10), 7834-7841.

59. Vyazovkin, S.; Burnham, A. K.; Criado, J. M.; Pérez-Maqueda, L. A.; Popescu, C.; Sbirrazzuoli, N., ICTAC Kinetics Committee recommendations for performing kinetic computations on thermal analysis data. *Thermochim. Acta* **2011,** 520, (1–2), 1-19.

60. Gilbert, R. G.; Ross, I. G., Concept of Activation Energy in Unimolecular

Reactions. *J. Chem. Phys.* **1972,** 57, (6), 2299-2305.

61. Vyazovkin, S., A time to search: finding the meaning of variable activation energy. *Phys. Chem. Chem. Phys.* **2016,** 18, (28), 18643.

62. Robertson, C. A.; Fryer, J. G., Some descriptive properties of normal mixtures. *Scand. Actuar. J.* **1969,** 1969, (3-4), 137-146.

63. Lai, Z.; Ma, X.; Tang, Y.; Lin, H., Thermogravimetric analysis of the thermal decomposition of MSW in N_2, CO_2 and CO_2/N_2 atmospheres. *Fuel Process. Technol.* **2012,** 102, 18-23.

64. Moyo, P. The application of a distributed activation energy based model to the gasification and combustion of coal and biomass char blends. University of Witwatersrand, Johannesburg, South Africa, 2013.

65. Ashman, K. M.; Bird, C. M.; Zepf, S. E., Detecting bimodality in astronomical datasets. *Astron. J.* **1994,** 108, (6), 2348-2361.

66. Cai, J.; He, Y.; Yu, X.; Banks, S. W.; Yang, Y.; Zhang, X.; Yu, Y.; Liu, R.; Bridgwater, A. V., Review of physicochemical properties and analytical characterization of lignocellulosic biomass. *Renewable Sustainable Energy Rev.* **2017,** 76, 309-322.

1
2
3
4
5
6
7
8
9
10
11
12
13
14
15
16
17
18
19
20
21
22
23
24
25
26
27
28
29
30
31
32
33
34
35
36
37
38
39
40
41
42
43
44
45
46
47
48
49
50
51
52
53
54
55
56
57
58
59
60

Graphical abstract